RSC Advances

PAPER

View Article Online
View Journal | View Issue

Open Access Article. Published on 13 April 2022. Downloaded on 11/8/2025 3:14:16 AM.
This article is licensed under a Creative Commons Attribution-NonCommercial 3.0 Unported Licence.

Check for updates

Cite this: *RSC Adv.*, 2022, **12**, 11591

Evaluation of the freshness of rainbow trout (*Oncorhynchus mykiss*) fillets by the NIR, E-nose and SPME-GC-MS

Kunli Xu,[a] Yuwen Yi,[b] Jing Deng,[b] Yuanhui Wang,[a] Bo Zhao,[a] Qianran Sun,[c] Chenhui Gong,[a] Zepeng Yang,[a] Hailun Wan,[a] Ruiyan He,[a] Xinyu Wu,[a] Bo Yao,[a] Meichao Zhang[a] and Yong Tang*[a]

Received 4th January 2022
Accepted 30th March 2022

DOI: 10.1039/d2ra00038e

rsc.li/rsc-advances

A comparison study on the freshness of rainbow trout (*Oncorhynchus mykiss*) fillets in the course of their sale was performed using near-infrared spectroscopy (NIRS), solid-phase microextraction combined with gas chromatography-mass spectrometry (SPME-GC-MS), and the electronic nose (E-nose) technique. Quantitative analysis of the volatile salt nitrogen (TVB-N) of rainbow trout fillets with different freshness using NIR combined with the partial least squares (PLS) method revealed that the predicted values of TVB-N of the samples were significantly correlated with the true values ($P < 0.01$). SPME-GC-MS combined with E-nose analysis demonstrated that there were significant differences in the volatile flavor components of rainbow trout fillets at different freshness, and E-nose combined with principal component analysis (PCA) and linear discriminant analysis (LDA) could achieve rapid and non-destructive freshness ranking of rainbow trout fillets based on volatile flavor characteristics. Consequently, the NIRS and E-nose non-destructive testing techniques are capable of acting as rapid screening tools for detecting the freshness of rainbow trout fillets during their sale.

1. Introduction

Rainbow trout (*Oncorhynchus mykiss*), which is widely promoted by the Food and Agriculture Organization of the United Nations (FAO), has become very popular among consumers worldwide. This is because they are not only rich in protein, polyunsaturated fatty acids, minerals, vitamins, and other nutrients, but also have high yields and high quality.[1–3] However, the abundant endogenous enzymes and psychrotrophic bacteria in rainbow trout, its fragile tissue structure, and large contact area with air during the selling process easily lead to a decline in the quality of rainbow trout.[4] The traditional method for the determination of freshness is usually based on sensory evaluation,[5–7] physical and chemical analysis (such as texture,[8,9] color variation,[10,11] and volatile salt nitrogen (TVB-N) produced by the hydrolysis of specific amino acids by microorganisms and enzymes[12,13]), microbiological testing,[14,15] *etc.* However, these methods are not only expensive, cumbersome, time-consuming, and destructive for the inspection of rainbow trout during their sale, but also difficult to meet the consumer requirements of fast and non-destructive testing of rainbow trout fillets. Definitely, these goals can be fulfilled using the near-infrared (NIR) and electronic nose (E-nose) non-destructive testing techniques, which have the advantages of high objectivity, fast detection, simple operation, good reproducibility and no requirement of complex sample pre-treatment.

NIR spectroscopy in the near-infrared spectral region (wavelength range of 780–2500 nm) is based on the multiplicative and synergistic absorption of organic hydrogen-containing groups (C–H, O–H, and N–H) by molecules, jumping from the ground to upper energy due to the non-harmonic vibrations of molecules.[16,17] NIR has been widely used in the evaluation of the quality and safety of meat and meat products in recent years.[18,19] de Nadai Bonin *et al.*[20] and Parastar *et al.*[21] used NIR combined with chemometric methods to achieve the rapid detection of intramuscular fat in beef and authenticity of chicken, respectively, both resulting in effective inspection and prediction.

Due to its high sensitivity and superior separation ability, solid-phase microextraction coupled with the gas chromatography-mass spectrometry method (SPME-GC-MS) has been widely used in the analysis of volatile and semi-volatile flavor components of foods. The E-nose is capable of sensing different volatile odor substances, where each sensor in the sensor array has interactive sensitivity with a high capacity to analyze and identify the overall characteristics of volatile flavor substances in food.[22,23] Zhang *et al.*[24] used PCA with E-nose and electronic tongue combined with SDE-GC-MS to effectively discriminate the different drying methods of golden pomfret.

[a]*School of Food and Biological Engineering, University of Xihua, Chengdu, Sichuan 610039, China. E-mail: jacktangy@gmail.com*

[b]*Cuisine Science Key Laboratory of Sichuan Province, University of Sichuan Tourism, Chengdu, Sichuan 610100, China*

[c]*Chengdu Esun Modern Technology Co., Ltd., Chengdu, Sichuan 610041, China*

© 2022 The Author(s). Published by the Royal Society of Chemistry

Open Access Article. Published on 13 April 2022. Downloaded on 11/8/2025 3:14:16 AM. This article is licensed under a Creative Commons Attribution-NonCommercial 3.0 Unported Licence.

Wang *et al.*[25] established an E-nose combined with GC-MS method to identify lamb adulterated with inferior duck meat, which makes these technologies have certain practical application value in the identification and reduction of adulterated meat samples. Xu *et al.*[26] reported that gas chromatography-time-of-flight mass spectrometry (GC-TOF-MS) and E-nose analysis revealed significant discrepancies in the content of volatile organic compounds (VOCs) in different parts of Chinese chicken, and subsequently combined with sensory evaluation showed that the flavor of chicken-like breast meat was superior to other parts. Adelina *et al.*[27] demonstrated that PCA combined with HS-SPME/GC-MS and E-nose showed superior separation of two grafted pines under different roasting conditions.

Herein, the present study addresses the issue of the lack of a time-sensitive and non-destructive rapid detection method in the marketing process of rainbow trout fillets to determine their quality. Using NIRS, SPME-GC-MS combined with E-nose, we were able to analyze the quality and safety of rainbow trout fillets. To investigate the quality change pattern of rainbow trout fillets during their sale, a rapid and non-destructive freshness measurement method was established with a positive significance on their quality, ensuring, economic value and additional value, and providing a reference for the safety of rainbow trout consumption and quality evaluation.

2. Materials and methods

2.1. Sample preparation

Freshly purchased rainbow trout was provided by Runzhao Fishery in 2020 (Tianquan, Yaan, Sichuan), with a mass of 3.5–4.5 kg per fish. After being executed in the laboratory, the head, tail, bone, and skin of all rainbow trout were removed and they were gutted, cleaned with distilled water, and cut into pieces of the same size (thickness 0.6 ± 0.1 cm and mass 10.0 ± 2.0 g). Subsequently, they were placed in trays and refrigerated at 4 °C, allowing the fillets to undergo natural decay in preparation for the subsequent determination and acquisition of their TVB-N values, NIR spectral information, GC-MS and E-nose fingerprinting information.

2.2. Determination of TVB-N values

The TVB-N values of the rainbow trout fillet samples were measured using the automatic Kjeldahl method with reference to the Food Safety Chinese standard GB 5009.228-2016 "Determination of volatile salt nitrogen in food",[28] and three parallel experiments were performed for each group.

2.3. Near-infrared spectral information acquisition

A SupNIR-2720 near-infrared analyzer (Polycom Technology Co. A, Ltd., Hangzhou, China) was used for spectral data acquisition in this experiment. The instrument was preheated for 30 min prior to the experiment, and then the instrument performance test was completed when it was stable, followed by calibration of the instrument with the reference white board. The rainbow trout fillets were removed from the 4 °C freezer, and then the surface water was absorbed using filter paper and the samples spread evenly in the test sample tray for rapid acquisition of NIR spectral information. The temperature of the spectral acquisition environment was 25 °C ± 2 °C, the humidity was 50% ± 5%, and the wavelength range of the instrument was 1000–1800 nm with a resolution of 12 nm. Each group consisted of 10 parallel samples, and to ensure a consistent light range, each parallel needed to reload samples of the same thickness 3 times, a total of 30 times.

2.4. SPME-GC-MS analytical methods

The rainbow trout fillets were minced in a centrifuge tube and homogenized with saturated NaCl in a ratio of 1 : 2, where the sodium salt was added to increase the ionic strength of the water sample, thus reducing the solubility of the analytes in the aqueous phase and improving the extraction efficiency.[29] Through optimization of the experimental conditions, the final solid-phase microextraction protocol was determined as follows: after the treated surimi supernatant was equilibrated by holding at 50 °C for 10 min, the samples were extracted by inserting a manual injection handle fitted with a polydimethylsiloxane/divinylbenzene (PDMS/DVB, 65 μm, 1 cm)-type extraction head at 50 °C for 40 min, and then resolved at 250 °C for 5 min at the GC inlet.

The chromatographic column was an HP-5 quartz capillary column (30 m × 0.32 mm, 0.25 μm) with helium as the carrier gas. GC-MS method: the flow rate was 1.00 mL min^{-1}; the inlet temperature was 250 °C, and the column was operated in non-split mode. The initial temperature of the column was held at 35 °C for 1 min, and the first stage was ramped up to 200 °C at 10 °C min^{-1} without holding and the second stage was ramped up to 280 °C at 20 °C min^{-1} and held for 5 min. MS method: the ionization mode was EI, the electron energy was 70 eV, the ion source temperature was 230 °C, the interface temperature was 260 °C, and the mass scan range was 35–500 *m*/*z*. For each sample, the composition of the volatiles was evaluated in terms of peak area percentage.[30]

2.5. E-nose detection

A PEN3 E-nose (Airsense Analytics, Germany) was used for the odor characterization of the rainbow trout fillets with 10 built-in selective metal oxide semiconductor sensors and Table 1 shows

Table 1 Features of the sensors used in the PEN3 electronic nose system

Sensor number	Sensor name	Main applications (gas detector)
S1	W1C	Aroma component
S2	W5S	Oxynitride
S3	W3C	Ammonia (aromatic component)
S4	W6S	Hydrogen
S5	W5C	Aromatic components of alkane
S6	W1S	Methane
S7	W1W	Sulfide
S8	W2S	Alcohols, aldehydes and ketones
S9	W2W	Aromatic and organic sulfide
S10	W3S	Alkanes

 © 2022 The Author(s). Published by the Royal Society of Chemistry

Open Access Article. Published on 13 April 2022. Downloaded on 11/8/2025 3:14:16 AM.
This article is licensed under a Creative Commons Attribution-NonCommercial 3.0 Unported Licence.

the types of sensitive substances corresponding to each sensor. The electronic nose detection was performed with slight modification according to Huang *et al.*[31] After weighing 4 g of rainbow trout fillet samples in a 20 mL headspace vial and sealing it, the samples were placed in a constant temperature water bath at 60 °C for 30 min, and then taken out for E-nose fingerprinting data acquisition by headspace injection, with each group of samples detected 8 times in parallel. The specific measurement parameters of the E-nose were set as follows: pre-sampling time of 5 s, measurement time of 90 s, flush time of 90 s, zero-point trim time of 10 s, measuring interval time of 1 s, chamber flow of 300 mL min^{-1}, and initial flow of 300 mL min^{-1}.

2.6. Data analysis

All statistical analysis was performed using SPSS 26.0 and plotted using Origin Pro 9.0. The analysis of the NIR spectral data was performed with the RIMP Client software, which came with the instrument. The analysis of volatile flavor substances was performed by controlled search in the NIST17 Spectral Library, where the substances with similarities greater than 80 were used as qualitative results, and the peak area normalization algorithm was used to calculate their relative percentage content for substance quantification. The E-nose data analysis was performed using its Winmuster software.

3. Results and discussion

3.1. Analysis of TVB-N values of rainbow trout fillets

The results of the TVB-N values of the rainbow trout fillets stored in a refrigerated room at 4 °C for 0–5 days are shown in Fig. 1, where the TVB-N values of the fillets continued to increase with an increase in storage time. The increase in alkaline nitrogenous substances such as ammonia and amines produced by the decomposition of proteins under the action of enzymes and microorganisms was caused by the increase in amino acid destruction in food with the extension of time.[32] According to the national food safety standard GB 2733-2015 "Fresh and Frozen Animal Fishery Products",[33] it is stipulated that the TVB-N value as the freshness index of animal food should not exceed 20 mg/100 g. As shown in Fig. 1, the TVB-N value of the rainbow trout fillets was 19.57 mg/100 g on the 2nd day, which reached the critical point of spoilage, while on the 5th day, the TVB-N value was as high as 29.05 mg/100 g. Accordingly, the freshness of rainbow trout fillets can be classified into three groups, as follows: fresh (TVB-N < 15 mg/100 g), sub-fresh (15 mg/100 g ≤ TVB-N ≤ 20 mg/100 g), and putrid (TVB-N > 20 mg/100 g).

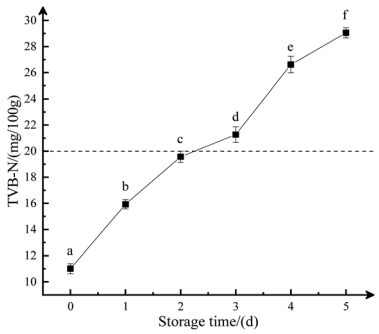

Fig. 1 Changes in TVB-N value of rainbow trout fillets with storage time.

3.2. NIR analysis

3.2.1 NIR spectra of rainbow trout fillets. Given that the NIR spectra coincide with the absorption regions of the ensemble frequencies and multiples of the vibration of hydrogen-containing groups in organic molecules, the characteristic information related to hydrogen-containing groups in the samples can be characterized. Fig. 2(a) shows the raw NIR spectra of the rainbow trout fillets stored in a refrigerated room at 4 °C for 0–5 days. The spectral curves of the rainbow trout fillet samples with a consistent overall trend but individual differences can be seen in Fig. 2(a), where there was a positive spectral response in the wavelength range of 1000–1800 nm. Among them, the intense absorption peaks appearing in the range of 1100 to 1400 nm are mainly the absorption bands of C–H bonds,[34] and the peaks in the range of 1450 to 1800 nm are mainly the characteristic absorption bands of the O–H groups.[35] Fig. 2(b) shows the average NIR spectra of the rainbow trout fillets with different freshness, where it can be seen that the spectral profiles of the rainbow trout fillets with different

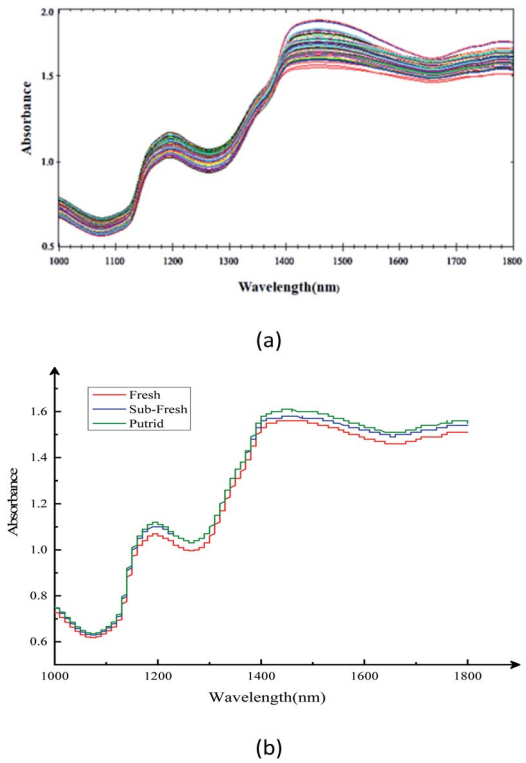

Fig. 2 NIR spectra of rainbow trout fillets: (a) original NIR spectra of rainbow trout fillets and (b) average NIR spectra of rainbow trout fillets with different freshness.

Open Access Article. Published on 13 April 2022. Downloaded on 11/8/2025 3:14:16 AM.
This article is licensed under a Creative Commons Attribution-NonCommercial 3.0 Unported Licence.

freshness were significantly different near 1500–1530 nm. Given that the vicinity of 1500–1530 nm mainly represents the first-order octave of the N–H bond stretching vibration,[36] the proteins in the rainbow trout fillets of different freshness were decomposed to different degrees, and the spectral absorption of the proteins was mainly related to the vibration of N–H groups, thus showing a significant difference in absorbance in this range.

3.2.2 Determination of the optimal pretreatment method. It is necessary to pre-process a spectrum before analysis to prevent interference factors (such as background noise, baseline drift, light range variation, and light scattering) in the spectral information of the sample from affecting the accuracy of the analysis results, which can enhance the valid information carried in the spectra.[37] The pretreatment methods used in this study are shown in Table 2.

According to the sample spread shown in Table 3, the overall range of TVB-N values of the samples was wide, covering the variation of values for the different freshness of the rainbow trout fillets, which was representative. The collected near-infrared spectral sample sets of rainbow trout fillets were divided into calibration and validation sets in the ratio of 3 : 1 according to the KS classification method, which was used to establish a quantitative model of TVB-N values of freshness index and to verify the accuracy of the model. The standard deviation of the calibration set (SEC), the correlation coefficient of the calibration set (RC), the standard deviation of the validation set (SEP), the correlation coefficient of the validation set (RP), and standard deviation of the K-fold interaction test set (SECV) were used as model accuracy evaluation parameters to predict the accuracy of the mean deviation test model. Among them, with smaller values of SEC and SEP, the more accurate the prediction of the model, the closer RC and RP are to 1, the better the correlation between the predicted and true values obtained by the model; and the smaller the SECV, the better the regressive model.[37]

As shown in Table 4, single and combined preprocessing methods were applied to build the quantitative PLS model with the raw spectral data as the blank control. The accuracy evaluation parameters of the model after SNV preprocessing were all good, with the smallest values of SEC and SECV, which indicated that the model had accurate prediction results and the best regression. The values of RC and RP were both greater than 0.95 and better than the model evaluation parameters without the pretreatment method, which indicated that there was a robust correlation between the predicted and true values. Fig. 3 shows the NIR spectra after SNV pre-processing. It can be seen that the SNV pre-processing used in the original NIR spectra of the rainbow trout fillets effectively weakened the influence of noise, scattering effects, and linear baseline drift on the spectra, while the spectral information of the characteristic bands was highlighted, which indicated that the model fitted the information in the spectrum and better reflected the TVB-N content of the rainbow trout fillets.[43] Thereby, it can be concluded that pre-processing the raw NIR spectra of rainbow trout fillets with SNV alone can enhance the model performance and improve the accuracy of the model prediction.

3.2.3 Quantitative modeling and analysis of TVB-N values. The quantitative model of TVB-N values in the rainbow trout fillets was developed using the SNV + PLS method. After substituting 45 validation set samples into the model for the determination of the TVB-N values, the relationship between the calibration set and validation set of the true values and predicted values was obtained, as shown in Fig. 4(a) and (b),

Table 2 Spectral preprocessing methods and effects

Spectral pre-processing method	Effects
Mean centering (MC)	Improves performance, while eliminating offset and avoiding numerical errors[38]
Savitzky–Golay smoothing (SGS)	Reduces the random noise caused by the system itself and improves the spectrum signal-to-noise ratio[39]
Savitzky–Golay derivative (SGD)	Removes baseline drift and improves the signal connected with organic compounds, highlighting characteristic spectra[40]
Standard normal variate transformation (SNV)	Reduces the influence of inhomogeneous sample particles, linear baseline drift, scattering effects, noise, and other factors on the spectrum[41]
Multiplication scatter correction (MSC)	Effectively reduces baseline compensation and multiplication effects and eliminates nonlinear baseline drift[42]

Table 3 The measured analysis of TVB-N value of rainbow trout fillets

		TVB-N/(mg/100 g)			
Sample	Sample size	Max	Min	Average value	Standard deviation
Total sample	180	29.776	10.708	20.370	6.165
Calibration	135	29.776	10.296	20.406	6.313
Validation	45	29.336	10.708	20.273	5.812

 © 2022 The Author(s). Published by the Royal Society of Chemistry

Open Access Article. Published on 13 April 2022. Downloaded on 11/8/2025 3:14:16 AM.
This article is licensed under a Creative Commons Attribution-NonCommercial 3.0 Unported Licence.

Table 4 Evaluation parameters of different pre-processing methods of the model

Pretreatment method	PLS components	Calibration set		Validation set		
		SEC	R_C	SEP	R_P	SECV
No pre-processing	14	0.4037	0.9981	1.5058	0.9604	1.3462
MC	14	0.3761	0.9985	1.4282	0.9694	1.2789
SGS 25-3[a]	14	0.9909	0.9887	1.3293	0.9739	1.4087
SGD 11-2-1[b]	9	0.8408	0.9915	1.3622	0.9724	1.3996
SNV	13	0.3209	0.9988	1.4314	0.9693	1.1496
MSC	11	0.6369	0.9952	1.4830	0.9671	1.3263
MC + SGD 11-2-1	9	0.8238	0.9919	1.3885	0.9715	1.3930
MC + SGS 25-3	14	0.9834	0.9891	1.5236	0.9651	1.3085
MC + SNV	9	1.8506	0.9540	3.5205	0.8803	2.3582
MC + MSC	4	5.9652	0.3542	5.3696	0.4048	9.1468
SGS 25-3 + SGD 11-2-1	10	0.9181	0.9898	1.4000	0.9707	1.3788
SGD 11-2-1 + SNV	9	0.8830	0.9907	1.3825	0.9714	1.4644
SGD 11-2-1 + MSC	9	0.8895	0.9905	1.3864	0.9712	1.4722
SGS 25-3 + SNV	14	0.9250	0.9900	1.3672	0.9720	1.2886
SGS 25-3 + MSC	14	0.9391	0.9897	1.3785	0.9715	1.3054
MC + SGD 11-2-1 + SGS 25-3	10	0.8919	0.9906	1.4266	0.9694	1.3276
MC + SGD 11-2-1 + SNV	6	1.7962	0.9595	1.6270	0.9605	2.0631
MC + SGD 11-2-1 + MSC	1	6.2676	0.1114	5.9062	0.2981	6.2378
MC + SGS 25-3 + SNV	11	1.8349	0.9567	3.6901	0.8611	2.1726
MC + SGS 25-3 + MSC	4	5.9708	0.3518	5.4062	0.3917	7.1418
SGD 11-2-1 + SGS 25-3 + SNV	10	0.9336	0.9899	1.4050	0.9704	1.3554
SGD 11-2-1 + SGS 25-3 + MSC	10	0.9382	0.9893	1.3097	0.9747	1.3790
MC + SGS 25-3 + SGD 11-2-1 + SNV	9	0.8959	0.9909	1.7215	0.9571	1.2067
MC + SGS 25-3 + SGD 11-2-1 + MSC	9	0.9777	0.9886	1.4028	0.9704	1.3830

[a] The window parameter of SGS algorithm was 25 and the number of fits was 3. [b] The window parameter of SGD algorithm was 11, the number of fits was 2, and the order of derivation was 1.

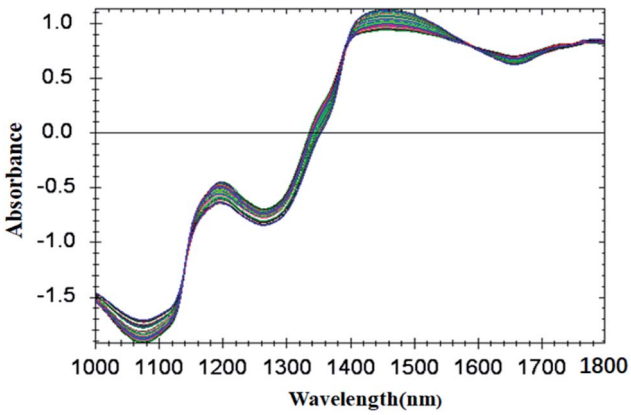

Fig. 3 NIR spectra after SNV pretreatment.

respectively. The distribution of sample points in both sets exhibits aggregation of each dispersion, which was caused by the significant daily variation in the TVB-N values of the rainbow trout fillets stored in a 4 °C freezer, resulting in uneven distribution of sample data. However, the model-predicted values of TVB-N in the two sets have a high correlation with the true values, with the average deviation of prediction being 6.14×10^{-5} and 0.26, respectively. This indicates that the model built by the SNV + PLS method has excellent prediction ability for the TVB-N values.

Aiming to predict the TVB-N freshness index of the rainbow trout fillets, the measured true TVB-N values of the 10 sample sets that were not involved in the modeling were imported into the established best model, and the model predictions were compared with the true values and determined by correlation analysis, and the results are shown in Table 5. The deviation of the average TVB-N prediction in the model for the external validation samples was 0.16, and the correlation coefficient between the predicted and true values was 0.969, indicating that the predicted values obtained from the model were significantly correlated with the true values and the model had a good predictive ability for the TVB-N freshness index of rainbow trout fillets.

3.3. SPME-GC-MS analysis

3.3.1 Total ion flow diagram of rainbow trout fillets of different freshness. SPME-GC-MS was used to examine the volatile flavor composition of the rainbow trout fillets with different freshness. According to Fig. 5, there were significant differences in the volatile profiles of the rainbow trout fillets in the three classes, where it can be seen that the relative content of volatile substance composition showed a significant increasing trend as the putridness of the rainbow trout fillets increased.

3.3.2 Analysis of the main volatile substance components of rainbow trout fillets of different freshness. The degree of protein decomposition and lipid oxidation of the rainbow trout

Open Access Article. Published on 13 April 2022. Downloaded on 11/8/2025 3:14:16 AM.
This article is licensed under a Creative Commons Attribution-NonCommercial 3.0 Unported Licence.

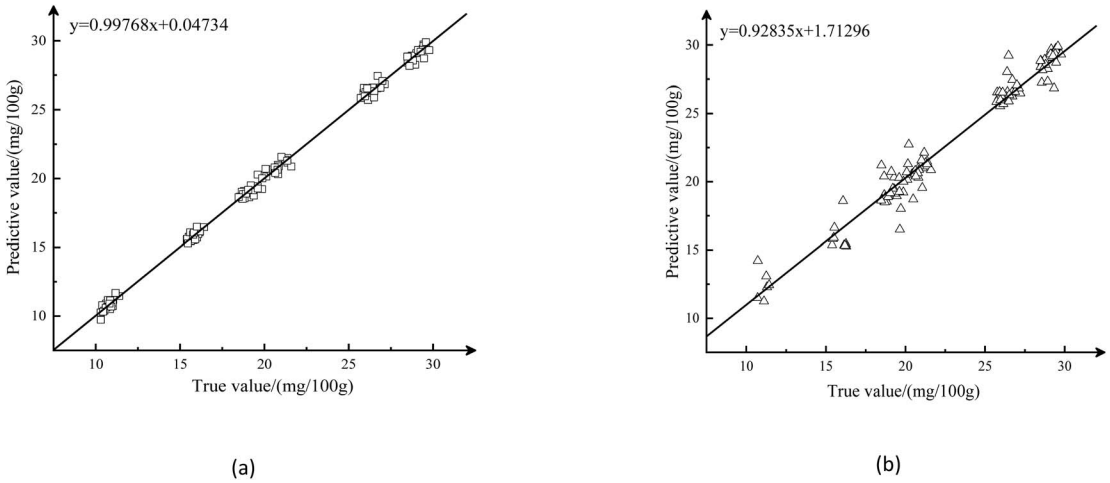

Fig. 4 Relationship between the TVB-N predicted value and the true value: (a) relationship between the TVB-N predicted value and the true value of the correction set and (b) relationship between the TVB-N predicted value and the true value of the verification set.

Table 5 External verification results of unknown samples

	TVB-N/(mg/100 g)		
External verification sample	True value	Predicted value	Deviation
1	11.302	12.292	0.990
2	11.436	12.437	1.001
3	15.776	15.897	0.121
4	19.227	19.129	−0.098
5	18.712	18.502	−0.210
6	21.752	18.708	−3.044
7	20.855	20.868	0.013
8	20.801	20.774	−0.027
9	26.476	29.234	2.758
10	29.008	29.103	0.095
Average value	19.535	19.694	0.160
Standard deviation	5.720	5.837	1.440
Correlation coefficient	0.969**		

fillets varied by freshness, which led to differences in the composition of the volatile substances.[44] The volatile flavor components of the rainbow trout fillets of different freshness were identified by GC-MS and the clustering heat of the main volatile components is shown in Table 6 and Fig. 6. There were 6 main categories of rainbow trout fillets with 88 volatile flavor substance components being identified in three different freshness (Table 6), including 47 hydrocarbons, 11 alcohols, 14 aldehydes, 1 acid, 4 ketones, and 11 esters. Among them, hexanal, nonanal, 1-octen-3-ol, and other major volatile substances were detected in fish.[45] However, only 7 of the identified substances were volatile components shared by the three freshness rainbow trout fillets, indicating that there are significant differences in the volatile flavor components contained in rainbow trout fillets with different freshness. The composition of substances that contributed significantly to the odor in the rainbow trout fillets are shown in Fig. 6, which included 20 substances such as 2,3,5,8-tetramethyldecane,

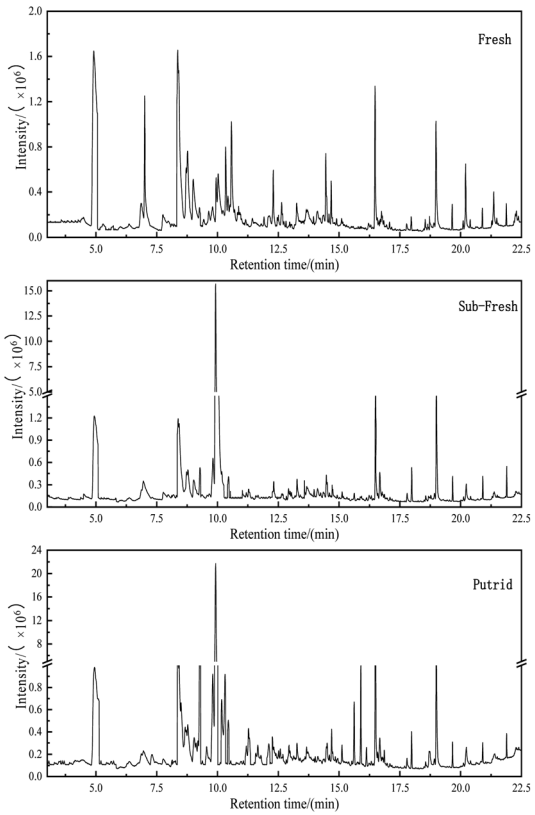

Fig. 5 Total ion current diagram of rainbow trout fillets with different freshness.

pentadecane, *N*-heptadecane, 1-octen-3-ol, hexanal, decanal, (*E*,*E*)-2,4-heptadienaln-octanal, octanal, (2*E*,4*E*)-deca-2,4-dienal, 2,3-octanedione and 2-amino-5-methylbenzoic acid. The higher color difference of the same substance indicated the greater difference in the abundance of the substance in the different samples. The clustering analysis showed that (2*E*,4*E*)-deca-2,4-dienal, and (*E*,*E*)-2,4-heptadienaln-octanal were clustered in

 © 2022 The Author(s). Published by the Royal Society of Chemistry

Open Access Article. Published on 13 April 2022. Downloaded on 11/8/2025 3:14:16 AM.
This article is licensed under a Creative Commons Attribution-NonCommercial 3.0 Unported Licence.

Table 6 GC-MS identification results of volatile components of rainbow trout fillets with different freshness[a]

Keep time/min	Compounds	Relative content/%		
		Fresh	Sub-fresh	Putrid
Hydrocarbons (47 types)				
6.020	(*Z*)-Tetradec-3-ene	0.24 ± 0.03	—	—
8.500	7-Methyl-3-methyleneocta-1,6-diene	—	—	4.47 ± 0.36
9.045	2,7-Dimethylocta-1,3,7-triene	—	—	2.22 ± 0.15
9.115	*cis*-1,1,3,5-Tetramethylcyclohexane	—	—	1.29 ± 0.06
9.195	1,2,4,5-Tetramethylbenzene	—	0.49 ± 0.02	—
9.260	(+)-Limonene	1.02 ± 0.04	—	10.32 ± 1.10
9.555	(*Z*)-β-Ocimene	—	—	0.65 ± 0.09
9.575	alpha-Ocimene	—	0.80 ± 0.05	—
9.640	2,3,5,8-Tetramethyldecane	1.44 ± 0.13	—	—
9.805	1-Bromo-3,7-dimethylocta-2,6-diene	—	—	5.81 ± 0.26
9.815	2,5-Dimethyl-2-hexene	—	4.99 ± 0.27	—
10.025	1-Tetradecen-3-yne	4.92 ± 0.33	—	—
10.170	2,5,5-Trimethyl-4-hydroxy-2,6-heptadien	—	—	3.73 ± 0.41
10.430	2,3,5,8-Tetramethyldecane	1.58 ± 0.29	—	2.01 ± 0.16
10.700	2,5-Dimethyl-6-methylidenespiro[2.4]heptane	1.09 ± 0.12	—	—
12.110	Dodecane	—	—	1.75 ± 0.18
12.130	(8*Z*,11*Z*,14*Z*)-Heptadeca-1,8,11,14-tetraene	0.72 ± 0.09	—	—
12.580	5-Ethylidene-1-methylcycloheptene	—	—	0.80 ± 0.04
13.050	5-Methyltetradecane	0.07 ± 0.02	—	—
13.255	1-Iodotetradecane	1.21 ± 0.14	2.14 ± 0.25	—
13.380	5-Methyl-5-propylnonane	0.73 ± 0.08	—	—
13.400	5-Butylnonane	—	0.69 ± 0.07	—
13.470	Dodecane,4,6-dimethyl	0.03 ± 0.00	—	—
13.580	5-(2-Methylpropyl)nonane	0.18 ± 0.02	—	—
13.650	Tridecane	0.87 ± 0.11	—	0.81 ± 0.06
13.675	1-Chlorohexadecane	—	1.20 ± 0.14	—
13.890	1-Iodo-decane	—	0.62 ± 0.07	—
13.950	Dodecane,4,6-dimethyl	0.47 ± 0.03	0.70 ± 0.04	0.33 ± 0.08
14.020	Isohexadecane	—	—	0.44 ± 0.05
14.240	2,6,10-Trimethyltridecane	—	0.90 ± 0.07	—
15.105	Tetradecane	0.62 ± 0.04	0.72 ± 0.03	—
15.120	1-Chlorooctadecane	—	—	0.92 ± 0.11
15.390	(1*R*,4*Z*,9*S*)-4,11,11-Trimethyl-8-methylidenebicyclo[7.2.0]undec-4-ene	—	—	0.39 ± 0.06
15.625	β-Caryophyllene	—	0.59 ± 0.09	—
16.215	4-Ethyl-3-nonen-5-yne	0.26 ± 0.04	—	—
16.390	1-Tetradecene	0.05 ± 0.01	—	—
16.400	1-Heptadecene	—	—	0.21 ± 0.01
16.405	1-Pentadecene	—	0.23 ± 0.04	—
16.475	Pentadecane	4.25 ± 0.26	—	6.60 ± 0.53
16.500	*N*-Heptadecane	0.27 ± 0.03	13.85 ± 1.19	5.02 ± 0.42
16.925	Icosane	—	0.36 ± 0.01	—
16.975	(+/−)-*trans*-Calamanene	—	0.29 ± 0.05	0.22 ± 0.03
17.325	1-Iodohexadecane	—	0.12 ± 0.03	—
17.790	Hexadecane	—	0.57 ± 0.05	0.41 ± 0.07
18.360	Pentacosane	—	0.07 ± 0.01	—
18.770	1-Heptadecene	—	0.35 ± 0.04	—
18.985	*N*-Heneicosane	4.55 ± 0.46	—	—
Alcohols (11types)				
8.365	Oct-1-en-3-ol	6.79 ± 0.33	6.31 ± 0.59	4.71 ± 0.27
9.435	2,4-Dimethylcyclohexan-1-ol	0.64 ± 0.08	1.81 ± 0.17	—
9.795	2-Octyn-1-ol	2.14 ± 0.32	—	—
10.040	*cis*-4-Thujanol	—	13.55 ± 1.17	—
10.310	2-[(2*R*,5*S*)-5-Methyl-5-vinyltetrahydro-2-furanyl]-2-propanol	—	—	4.82 ± 0.36
11.280	*cis*-Sabinol	—	1.47 ± 0.22	—
11.315	(1alpha,2alpha,5alpha)-2-Methyl-5-(1-methyl-ethyl)bicyclo[3.1.0]hexan-2-ol	—	—	1.02 ± 0.09
13.270	Cyclooctanol	—	—	1.43 ± 0.16
14.365	Cerotin	1.06 ± 0.07	—	—
18.250	(+)-Cedrol	—	0.05 ± 0.00	—
18.920	2-Hexyl-1-decanol	—	0.71 ± 0.06	0.45 ± 0.04

Open Access Article. Published on 13 April 2022. Downloaded on 11/8/2025 3:14:16 AM.
This article is licensed under a Creative Commons Attribution-NonCommercial 3.0 Unported Licence.

Table 6 (*Contd.*)

Keep time/min	Compounds	Relative content/%		
		Fresh	Sub-fresh	Putrid
Aldehydes (14 types)				
4.915	Hexanal	22.40 ± 1.41	4.65 ± 0.31	17.19 ± 1.06
6.005	*trans*-2-Hexenal	—	0.17 ± 0.01	—
6.860	Heptanal	2.46 ± 0.18	—	—
6.870	Decanal	—	1.77 ± 0.09	1.95 ± 0.06
7.950	Heptenal	0.84 ± 0.06	—	0.36 ± 0.02
8.715	(*E*,*E*)-2,4-Heptadienal	7.74 ± 0.57	7.62 ± 0.61	1.42 ± 0.13
8.765	Octanal	5.63 ± 0.29	4.60 ± 0.34	3.89 ± 0.15
10.570	Nonanal	5.15 ± 0.20	—	—
11.180	alpha-Cyclocitral	—	—	1.19 ± 0.03
13.695	(2*E*,4*E*)-Deca-2,4-dienal	3.40 ± 0.25	1.81 ± 0.17	—
13.840	Undecanal	—	0.51 ± 0.06	0.41 ± 0.04
14.110	(*E*,*E*)-2,4-Dodecadienal	—	1.92 ± 0.11	—
15.310	Tridecanal	0.25 ± 0.03	—	0.35 ± 0.04
15.320	Lauryl aldehyde	—	0.43 ± 0.08	—
Acids (1 type)				
7.005	2-Amino-5-methylbenzoic acid	5.73 ± 0.26	5.83 ± 0.15	—
Ketones (4 types)				
8.405	2,3-Octanedione	10.33 ± 0.53	10.70 ± 0.68	5.04 ± 0.42
11.160	1-(Furan-2-yl)butan-2-one	0.19 ± 0.06	—	—
11.580	1-Propan-2-ylbicyclo[3.1.0]hexan-4-one	—	0.12 ± 0.03	0.68 ± 0.08
13.135	3-Methyl-6-(1-methylethyl)-2-cyclohexen-1-one	—	—	0.67 ± 0.10
Esters (11 types)				
7.315	Methyl hexanoate	—	—	1.48 ± 0.12
8.670	Ethyl hexanoate	—	—	2.23 ± 0.17
9.280	(*Z*)-3,7-Dimethyl-2,7-octadien-1-yl propanoate	—	2.59 ± 0.15	—
10.175	Methyl 5-oxooxolane-2-carboxylate	—	3.34 ± 0.21	—
11.275	(1*S*,3*R*,5*S*)-4-Methylidene-1-(propan-2-yl)bicyclo[3.1.0]hex-3-yl acetate	—	—	1.55 ± 0.18
12.360	*n*-Propyl methacrylate	—	—	0.46 ± 0.07
14.825	(3-Hydroxy-2,2,4-trimethylpentyl) 2-methylpropanoate	0.26 ± 0.01	—	—
15.020	Nonyl-2,2,2-trichloroacetat	—	0.38 ± 0.04	—
17.695	2,2,4-Trimethyl-1,3-pentanediol diisobutyrate	—	—	0.10 ± 0.00
18.895	Nonyl-2-methylpropanoate	0.33 ± 0.03	—	—
20.625	Diisobutyl phthalate	0.10 ± 0.00	—	0.22 ± 0.01

[a] "—" means not detected.

one group and tridecane, 2,3,5,8-tetramethyldecane and pentadecane were clustered in another group, which may be because they showed some correlation in the volatile odor of rainbow trout fillets.

The composition and content of the volatile flavor substances of the rainbow trout fillets of different freshness are shown in Table 7 and Fig. 7. In the rainbow trout fillets of different freshness, 38, 40, and 42 volatile flavor substance components were identified, respectively, where hydrocarbon compounds were the highest number of volatile profiles classified in all the rainbow trout fillet samples, followed by aldehydes. Furthermore, the changes in hydrocarbons, alcohols, and aldehydes were more pronounced in the rainbow trout fillets from freshness to putridness than that in the other three compounds.

The production of hydrocarbons is mainly attributed to the homogeneous cleavage of fatty acid alkoxy radicals. In the detection of volatile flavor substances in the rainbow trout fillets of different freshness, hydrocarbons were the most diverse, including alkanes, olefins, and alkynes, and their average relative content was 34.20%, the highest among the substance types. It has been found that various alkanes (C6 to C19) are present in the volatile composition of fish and have the effect of enhancing the overall flavor of fish.[44] In this experiment, a total of 20 hydrocarbons were detected in the fresh rainbow trout fillets. Among them, 14 alkanes were detected, being the most volatile category, and mainly concentrated between C7 and C21, where the relative contents of pentadecane and *n*-heneicosane were higher, in accordance with the results by Josephson *et al.*[46]

 © 2022 The Author(s). Published by the Royal Society of Chemistry

Open Access Article. Published on 13 April 2022. Downloaded on 11/8/2025 3:14:16 AM.
This article is licensed under a Creative Commons Attribution-NonCommercial 3.0 Unported Licence.

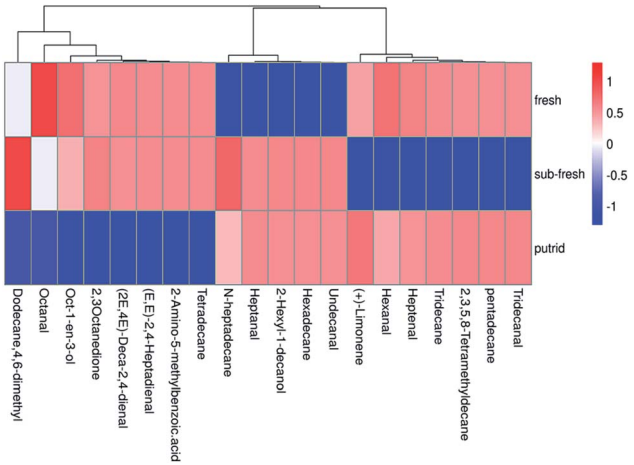

Fig. 6 Heatmap of main volatile flavor components of rainbow trout fillets with different freshness.

Alcohols are mainly produced by the oxidative decomposition of lipids and some come from the reduction of carbonyl compounds (such as aldehydes and ketones). The accumulation of some alcoholic volatile components was caused by the metabolism of putrid microorganisms, mainly by the oxidation of polyunsaturated fatty acids.[47] The average relative content of alcohols in the detection of volatile flavor substances among the rainbow trout fillets of different freshness was 20.43%, and the relative content showed a stable increasing trend from freshness to putridness. This indicated that alcohols explained the flavor of the putrid rainbow trout fillets to some extent. A small amount of *cis*-sabinol was detected in the sub-fresh rainbow trout fillets, but not in the putrid rainbow trout fillets, which may be due to the fact that the metabolites produced during the onset of putridness can be further metabolized by microorganisms.[48]

Aldehydes were one of the main volatile species in the rainbow trout fillets, and they had a lower flavor threshold than alcohols. The test results of the volatiles indicated that 14 types of aldehydes were detected, more than alcohols, but their average relative content was 27.94%, lower than that of alcohols. Similar results were found for French rainbow trout samples.[49] These samples also showed a significant decreasing trend as the freshness of the rainbow trout fillets decreased, which indicated that aldehydes contributed more to the aroma and characterized the flavor of fresh rainbow trout fillets.[50] Among them, hexanal was one of the most abundant carbonyl compounds in the fresh fish, and it produced a green plant-like aroma within seconds after death.[51] In addition, heptanal, *n*-octanal, and nonanal have also been reported to be present in fresh fish.[52] However, (*E*,*E*)-2,4-heptadienal detected in aldehydes has been considered as an important correlate of the fishy taste and its formation has been associated with the oxidation of polyunsaturated fatty acids in fish.[53]

The detection of volatile flavor substances in rainbow trout fillets of different freshness was low for acids, ketones, and esters, with 1, 4, and 11 compounds, respectively. The production of ketones may be due to the thermal oxidation or degradation of unsaturated fatty acids,[54] which had a much higher threshold than aldehydes, and therefore contributed relatively little to the fish odor. Among them, the detected 2,3-octanedione showed an "inverted V" trend, which may be representative of the transition from freshness to putrid in fish, in agreement with the results by Duflos *et al.*[55] In contrast, esters were less in type and relative content in the raw fish fillets, probably because esters need to accumulate under high-temperature conditions.

3.4. Rapid nondestructive testing of rainbow trout fillets by E-nose for freshness grading

3.4.1 E-nose sensor response analysis. A non-destructive rapid inspection technique of freshness grading based on volatile flavor characteristics was investigated utilizing the E-nose by comparing the differences in the volatile substance composition of rainbow trout fillets with different freshness. The non-destructive rapid inspection of rainbow trout fillet freshness by the E-nose utilizes the differential response of gas-sensitive sensors to the volatile flavor characteristics of rainbow trout fillets of different freshness.[56] The radar plot permits visualization and analysis of the multidimensional data of the E-nose in a two-dimensional graph.[57]

As shown in Fig. 8, the response trend of the E-nose to the rainbow trout fillet samples with different freshness was consistent, but the freshness of three rainbow trout fillet samples has obvious pattern differences. The response of the sensor to rainbow trout fillets with different freshness was strong to weak in order from putrid > sub-fresh > fresh, which was because the putrid rainbow trout fillets had a more intense

Table 7 Distribution of various volatile components in rainbow trout fillets with different freshness

Ingredient category	Classification number/species (relative content/%)			Average relative content/%
	Fresh	Sub-fresh	Putrid	
Hydrocarbons	20 (24.55)	19 (29.67)	20 (48.38)	34.20
Alcohols	4 (10.64)	6 (23.89)	5 (26.77)	20.43
Aldehydes	8 (47.87)	9 (23.47)	8 (12.47)	27.94
Acids	1 (5.73)	1 (5.83)	0 (0.00)	3.85
Ketones	2 (10.51)	2 (10.82)	3 (6.39)	9.24
Esters	3 (0.7)	3 (6.32)	6 (6.03)	13.05
Total	38	40	42	

Open Access Article. Published on 13 April 2022. Downloaded on 11/8/2025 3:14:16 AM.
This article is licensed under a Creative Commons Attribution-NonCommercial 3.0 Unported Licence.

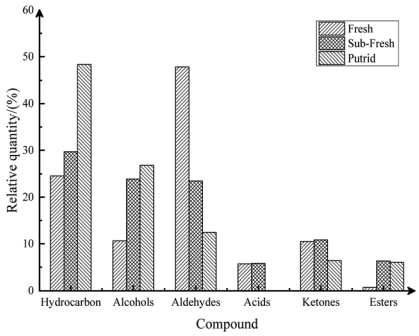

Fig. 7 Comparison of the content of various volatile substances in rainbow trout fillets with different freshness.

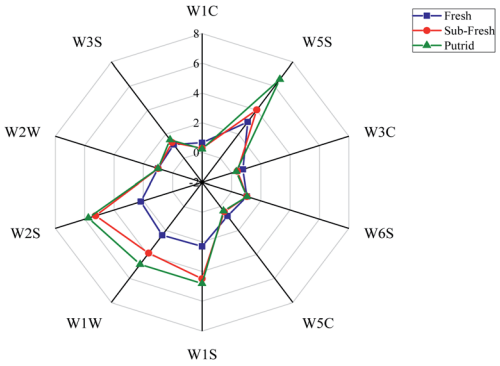

Fig. 8 Radar chart of E-nose sensor response to rainbow trout fillets with different freshness.

and abundant volatile odor than the sub-fresh and fresh fillets. Fig. 9 presents a histogram containing a comparative analysis of the E-nose sensor response values for rainbow trout fillets with different freshness based on the radar plot. The response of W5S, W1S, W1W, and W2S to the rainbow trout fillet samples was stronger than that of the other six sensors, and there were significant differences among the different freshness groups. This result indicates that the volatile odor substances of the rainbow trout fillets were mainly nitrogen oxides, alkanes, sulfides, alcohols, and other aromatic components.

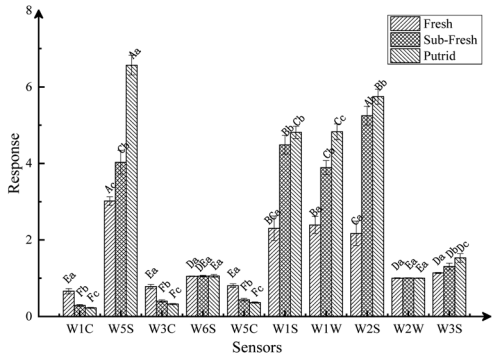

Fig. 9 Bar graph of response value of E-nose sensor for rainbow trout fillets with different freshness.

3.4.2 Loading analysis. The loading analysis represents the loading factors associated with the first and second principal components of each sensor.[58] The scattered points in Fig. 10 represent 10 different sensors with coordinate distances, explaining the magnitude of the contribution of each sensor to the sample differentiation and the type of volatiles that subsequently play a major role in the sample differentiation. The contributions of the first and second principal components were 90.74% and 6.77%, respectively, with a total contribution of 97.51%, which can represent the main characteristic information of the rainbow trout fillet samples. W2S, W5S, W1C, and W1W contributed more to the first principal component than the other sensors and played a major role in distinguishing the volatile odors of the rainbow trout fillets with different freshness. Also, W1S contributed more to the second principal component and played a secondary role in distinguishing the volatile odors of the rainbow trout fillets with different freshness, while the coordinates of the W2W, W6S and W3S sensors were close to zero point (0,0) and contributed less to both the first and second principal components, which indicated they played a smaller role in identifying the volatile odors of the rainbow trout fillets.[59]

3.4.3 PCA analysis and LDA analysis. PCA is an unsupervised method for dimensionality reduction classification. Based on the premise of retaining as much information as possible, a multidimensional vector was mapped to a low-dimensional space by an orthogonal transformation.[60] The data matrix of the response values of the rainbow trout fillets of different freshness using the E-nose sensor array was subjected to principal component analysis, and the results are shown in Fig. 11, where the contributions of PC-1 and PC-2 were 90.74% and 6.77%, respectively, with a cumulative contribution of 97.51%, which could effectively distinguish the changes in the volatile odor characteristics of the rainbow trout fillets.[61] Also, there was no overlapping area between the three different freshness samples, indicating that the freshness of the rainbow trout fillets could be clearly distinguished using the E-nose.

Linear discriminant analysis (LDA) is the projection of high-dimensional sample signal data into a low-dimensional space with good categorical differentiability to maximize the ratio of between-group differences to within-group differences.[62,63] Fig. 12 shows the LDA of the rainbow trout fillets with different

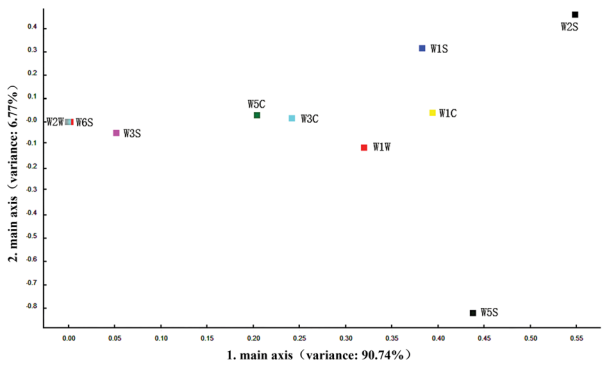

Fig. 10 Load analysis of E-nose sensor.

 © 2022 The Author(s). Published by the Royal Society of Chemistry

Open Access Article. Published on 13 April 2022. Downloaded on 11/8/2025 3:14:16 AM.
This article is licensed under a Creative Commons Attribution-NonCommercial 3.0 Unported Licence.

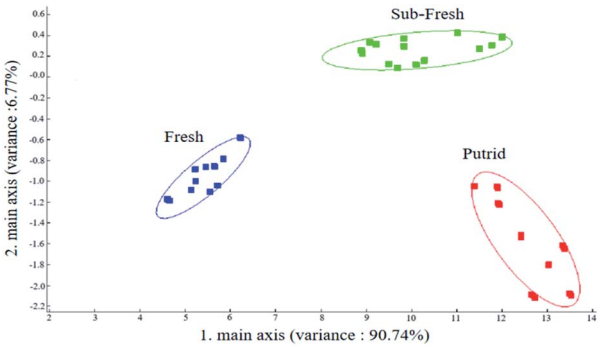

Fig. 11 Principal component analysis diagram of rainbow trout fillets with different freshness.

freshness, which had a better differentiation effect than PCA because the linear discriminant minimized the intra-group variation. As shown in Fig. 12, the contributions of LDA-1 and LDA-2 were 66.40% and 23.97%, respectively, with a cumulative contribution of 90.37%, which can represent the main information of the rainbow trout fillets. The E-nose combined with LDA was effective in distinguishing rainbow trout fillets of different freshness, where the samples of the fresh rainbow trout fillets were farther away from that of the sub-fresh and putrid rainbow trout fillets, which indicates that the volatile odor of the fresh rainbow trout fillets was very different than that of the other two freshness.

According to the research results of the E-nose combined with radar plot analysis, load analysis, PCA and LDA analysis of the rainbow trout fillets with different freshness, it can be concluded that the variations in nitrogen oxides, alkanes, sulfides, alcohols, and other aromatic compounds play a major role in distinguishing the volatile odors of the rainbow trout fillets, and further validate the results of the SPME-GC-MS analysis of volatile flavor substances of the rainbow trout fillets with different freshness. Meanwhile, the results indicate that the E-nose could realize the non-destructive rapid inspection of freshness grading based on the volatile flavor characteristics of rainbow trout fillets, which provides another new idea for non-destructive rapid inspection technology of freshness.

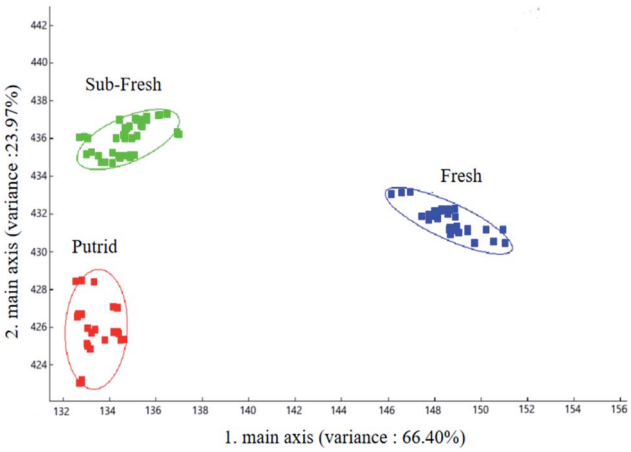

Fig. 12 Linear discriminant analysis diagram of rainbow trout fillets with different freshness.

4. Conclusions

The results of the linear regression fitting analysis based on NIR combined with PLS showed that there was a good correlation between the true and predicted values of TVB-N for the different freshness of rainbow trout fillets during the pending sale process. The composition and content of volatile flavor substances in the rainbow trout fillets of three different freshness were found to be very different based on SPME-GC-MS, and the detected main compounds were highly correlated with the response of the E-nose sensors. It was also demonstrated that the E-nose combined with PCA and LDA could achieve rapid non-destructive freshness grading of fresh, sub-fresh, and putrid rainbow trout fillets based on their volatile flavor characteristics, which provides a new thought for freshness non-destructive rapid inspection technology.

Author contributions

Conceptualization, Bo Zhao, Yuanhui Wang and Kunli Xu; data curation, Bo Zhao and Kunli Xu; formal analysis, Yuanhui Wang; funding acquisition, Yong Tang; investigation, Hailun Wan, Qianran Sun, Chenhui Gong, Ruiyan He, Xinyu Wu and Bo Yao; methodology, Kunli Xu; project administration, Chenhui Gong and Meichao Zhang; resources, Yuwen YI, Jing Deng, and Yong Tang; software, Zepeng Yang; supervision, Qianran Sun; visualization, Zepeng Yang and Meichao Zhang; writing – original draft, Kunli Xu and Bo Zhao; writing – review & editing, Kunli Xu and Yong Tang.

Conflicts of interest

The authors declare no conflict of interest.

Acknowledgements

This work was supported by the Chunhui Project of the Ministry of Education (Grant No. Z2016142); the Key R&D projects of the Department of Science and Technology of Sichuan Province (Grant No. 2020YFN0022); the Key R&D Projects of the Department of Science and Technology of Zhejiang Province (Grant No. 2019C02075); Project of Science and Technology Department of Sichuan Province (Grant No. 2020YFH0130); the Innovation and Entrepreneurship Program for College Students (Grant No. S201910622061).

References

1 L. Xiao, *Effect of temperature fluctuation during circulation on quality change and microbial diversity of bigorder tuna*, Shanghai Ocean University, Shanghai, 2018.

Open Access Article. Published on 13 April 2022. Downloaded on 11/8/2025 3:14:16 AM. This article is licensed under a Creative Commons Attribution-NonCommercial 3.0 Unported Licence.

2 Q. He, Z. Li, Z. Yang, Y. Zhang and J. Liu, *Aquaculture*, 2020, **514**, 734506.
3 M. M. Reis, E. Martínez, E. Saitua, R. Rodríguez, I. Pérez and I. Olabarrieta, *Lebensm.-Wiss. Technol.*, 2017, **78**, 129–137.
4 L. Wu, H. Pu and D. W. Sun, *Trends Food Sci. Technol.*, 2019, **83**, 259–273.
5 S. O. Knowles, N. D. Grace, J. R. Rounce and C. E. Realini, *Food Res. Int.*, 2020, **137**, 109655.
6 J. Zhang, B. Bowker, Y. Yang, B. Pang and H. Zhuang, *Lebensm.-Wiss. Technol.*, 2020, **120**, 108939.
7 D. P. Green, *Handb. Seafood Qual., Saf. Health Appl.*, 2010, 29–38.
8 A. Aussanasuwannakul, S. D. Slider, M. Salem, J. Yao and P. Brett Kenney, *J. Food Sci.*, 2012, **77**, S335–S341.
9 J. H. Cheng, D. W. Sun, Z. Han and X. A. Zeng, *Compr. Rev. Food Sci. Food Saf.*, 2014, **13**, 52–61.
10 Y. H. Kim, J. T. Keeton, H. S. Yang, S. B. Smith, J. E. Sawyer and J. W. Savell, *Meat Sci.*, 2009, **82**, 234–240.
11 D. J. Livingston and W. D. Brown, *Food Technol.*, 1981, **35**, 238–252.
12 Y. Zhang, Q. Luo, K. Ding, S. G. Liu and X. Shi, *Sens. Actuators, B*, 2021, **335**, 129708.
13 Y. Li, X. Tang, Z. Shen and J. Dong, *Food Chem.*, 2019, **287**, 126–132.
14 A. Naila, S. Flint, G. C. Fletcher, P. J. Bremer, G. Meerdink and R. H. Morton, *Food Chem.*, 2012, **135**, 2650–2660.
15 L. Huang, J. Zhao, Q. Chen and Y. Zhang, *Food Res. Int.*, 2013, **54**, 821–828.
16 M. Zareef, Q. Chen, M. Hassan, M. Arslan, M. M. Hashim, W. Ahmad, F. Kutsanedzie and A. A. Agyekum, *Food Eng. Rev.*, 2020, **12**, 173–190.
17 K. B. Beć, J. Grabska and C. W. Huck, *Chem.–Eur. J.*, 2021, **27**, 1514–1532.
18 S. Savoia, A. Albera, A. Brugiapaglia, L. Di Stasio, A. Ferragina, A. Cecchinato and G. Bittante, *Meat Sci.*, 2020, **161**, 108017.
19 M. Á. Fernández-Barroso, S. Parrini, M. Muñoz, P. Palma-Granados, G. Matos, L. Ramírez, A. Crovetti, J. M. García-Casco and R. Bozzi, *J. Food Compos. Anal.*, 2021, **102**, 104018.
20 M. de Nadai Bonin, S. da Luz e Silva, L. Bünger, D. Ross, G. L. Dias Feijó, R. da Costa Gomes, F. Palma Rennó, M. H. de Almeida Santana, F. Marcondes de Rezende, L. C. Vinhas Ítavo, F. J. de Novais, L. M. A. Surita, M. de Nadai Bonin, M. W. Filgueira Pereira and J. B. S. Ferraz, *Meat Sci.*, 2020, **163**, 108077.
21 H. Parastar, G. van Kollenburg, Y. Weesepoel, A. van den Doel, L. Buydens and J. Jansen, *Food Control*, 2020, **112**, 107149.
22 H. Zeng, Q. Li and Y. Gu, *Chin. Phys. B*, 2016, **25**, 024201.
23 M. Ghasemi-varnamkhasti and M. Aghbashlo, *Trends Food Sci. Technol.*, 2014, **38**, 158–166.
24 J. Zhang, J. Cao, Z. Pei, P. Wei, D. Xiang, X. Cao, X. Shen and C. Li, *Food Res. Int.*, 2019, **123**, 217–225.
25 Q. Wang, L. Li, W. Ding, D. Zhang, J. Wang, K. Reed and B. Zhang, *Food Control*, 2019, **98**, 431–438.
26 Y. Xu, Y. P. Chen, S. Deng, C. Li, X. Xu, G. Zhou and Y. Liu, *Food Res. Int.*, 2020, **137**, 109669.
27 N. M. Adelina, H. Wang, L. Zhang and Y. Zhao, *Food Res. Int.*, 2021, **140**, 110026.
28 *GB 2009.228-2016, Determination of Volatile base Nitrogen in Food*, Standards Press of China, Beijing, 2016.
29 J. Pawliszyn, Z. Zhang and T. Gorecki, *Theory and Practice of Solid Phase Microextraction*, Federation of Analytical Chemistry, United States, 1995.
30 E. Kafkas, T. Cabaroglu, S. Selli, A. Bozdoğan, M. Kürkçüoğlu, S. Paydaş and K. H. C. Başer, *Flavour Fragrance J.*, 2006, **21**, 68–71.
31 X. H. Huang, L. B. Qi, B. S. Fu, Z. H. Chen, Y. Y. Zhang, M. Du, X. P. Dong, B. W. Zhu and L. Qin, *Food Chem.*, 2019, **286**, 241–249.
32 A. E. D. A. Bekhit, B. W. B. Holman, S. G. Giteru and D. L. Hopkins, *Sci. Technol.*, 2021, **109**, 280–302.
33 *GB 2733-2015, Fresh and Frozen Animal Aquatic Products*, Standards Press of China, Beijing, 2015.
34 M. Qassem and P. A. Kyriacou, *J. Biomed. Opt.*, 2014, **19**, 87007.
35 N. Prieto, R. Roehe, P. Lavín, G. Batten and S. Andrés, *Meat Sci.*, 2009, **83**, 175–186.
36 X. Yu, J. Wang, S. Wen, J. Yang and F. Zhang, *Biosyst. Eng.*, 2019, **178**, 244–255.
37 Seema, A. K. Ghosh, B. S. Das and N. Reddy, *Geoderma Regional*, 2020, **23**, e00349.
38 M. Juybar, M. Khanmohammadi Khorrami, A. Bagheri Garmarudi and S. Zandbaaf, *Spectrochim. Acta, Part A*, 2020, **228**, 117539.
39 S. Weng, B. Guo, P. Tang, X. Yin, F. Pan, J. Zhao, L. Huang and D. Zhang, *Spectrochim. Acta, Part A*, 2020, **230**, 118005.
40 H. Jiang, Y. Ru, Q. Chen, J. Wang and L. Xu, *Spectrochim. Acta, Part A*, 2021, **249**, 119307.
41 H. Jiang, X. Jiang, Y. Ru, J. Wang, L. Xu and H. Zhou, *Infrared Phys. Technol.*, 2020, **110**, 103467.
42 T. Tiecher, J. M. Moura-Bueno, L. Caner, J. P. G. Minella, O. Evrard, R. Ramon, G. Naibo, C. A. P. Barros, Y. J. A. B. Silva, F. F. Amorim and D. S. Rheinheimer, *Geoderma*, 2021, **384**, 114815.
43 A. A. Agyekum, F. Y. H. Kutsanedzie, V. Annavaram, B. K. Mintah, E. K. Asare and B. Wang, *Vib. Spectrosc.*, 2020, **108**, 103044.
44 J. Iglesias and I. Medina, *J. Chromatogr. A*, 2008, **1192**, 9–16.
45 D. Yu, Y. Xu, J. M. Regenstein, W. Xia, F. Yang, Q. Jiang and B. Wang, *Food Chem.*, 2018, **242**, 412–420.
46 D. B. Josephson, R. C. Lindsay and D. A. Stuiber, *J. Food Sci.*, 1987, **52**, 596–600.
47 F. F. Parlapani, A. Mallouchos, S. A. Haroutounian and I. S. Boziaris, *Int. J. Food Microbiol.*, 2014, **189**, 153–163.
48 F. Leduc, P. Tournayre, N. Kondjoyan, F. Mercier, P. Malle, O. Kol, J. L. Berdagué and G. Duflos, *Food Chem.*, 2012, **131**, 1304–1311.
49 S. Selli, C. Prost and T. Serot, *Food Chem.*, 2009, **114**, 317–322.
50 C. Alasalvar, K. D. A. Taylor and F. Shahidi, *J. Agric. Food Chem.*, 2005, **53**, 2616–2622.
51 D. Josephson and R. Lindsay, *Biogeneration of Aromas*, T. H. Parliament and R. Croteau, 1155 Sixteenth

 © 2022 The Author(s). Published by the Royal Society of Chemistry

Open Access Article. Published on 13 April 2022. Downloaded on 11/8/2025 3:14:16 AM.
This article is licensed under a Creative Commons Attribution-NonCommercial 3.0 Unported Licence.

Street N.W.Washington, DC, United States of America, 1986, pp. 201–219.
52 T. Kawai and M. Sakaguchi, *Crit. Rev. Food Sci. Nutr.*, 1996, **36**, 257–298.
53 C. F. Ross and D. M. Smith, *Compr. Rev. Food Sci. Food Saf.*, 2006, **5**, 18–25.
54 Y. J. Cha, K. R. Cadwallader and H. H. Baek, *J. Food Sci.*, 1993, **58**, 525–530.
55 G. Duflos, F. Leduc, A. N'Guessan, F. Krzewinski, O. Kol and P. Malle, *J. Sci. Food Agric.*, 2010, **90**, 2568–2575.
56 J. Tan and J. Xu, *Artif. Intell. Med.*, 2020, **4**, 104–115.
57 S. Trirongjitmoah, Z. Juengmunkong, K. Srikulnath and P. Somboon, *Comput. Electron. Agric.*, 2015, **113**, 148–153.
58 H. Zhang, J. Wang, X. Tian, H. Yu and Y. Yu, *J. Food Eng.*, 2007, **82**, 403–408.
59 A. H. Gómez, J. Wang, G. Hu and A. G. Pereira, *Sens. Actuators, B*, 2006, **113**, 347–353.
60 H. Yu, Y. Wang and J. Wang, *Sensors*, 2009, **9**, 8073–8082.
61 Z. Wei, J. Wang and W. Zhang, *Food Chem.*, 2015, **177**, 89–96.
62 M. Ghasemi-Varnamkhasti, M. Tohidi, P. Mishra and Z. Izadi, *Postharvest Biol. Technol.*, 2018, **138**, 134–139.
63 Radi, S. Ciptohadijoyo, W. S. Litananda, M. Rivai and M. H. Purnomo, *Comput. Electron. Agric.*, 2016, **121**, 429–435.